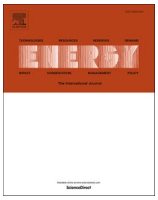
Energy 291 (2024) 130171



Contents lists available at ScienceDirect

Energy

journal homepage: www.elsevier.com/locate/energy





Data-driven compressor performance maps and cost correlations for small-scale heat-pumping applications

Andreas V. Olympios [a], Jian Song [a,b], Aleksander Ziolkowski [a], Vethalingam S. Shanmugam [a], Christos N. Markides [a,*]

[a] Clean Energy Processes (CEP), Laboratory and Sargent Centre for Process Systems Engineering, Department of Chemical Engineering, Imperial College London, London SW7 2AZ, UK

[b] Birmingham Centre for Energy Storage & School of Chemical Engineering, University of Birmingham, Birmingham ,B15 2TT, UK

ARTICLE INFO

Handling editor: Henrik Lund

Keywords:
Compressor
Data-driven
Heat pump
Isentropic efficiency
Optimisation
Technoeconomic

ABSTRACT

The performance of vapour-compression heat pumps depends crucially upon compressor selection and design. In this work, a unified modelling framework is developed to enable technoeconomic comparisons of compressors intended for small-scale heating applications (<30 kW_{th}). Published information on 120 commercially available compressors is analysed and used to develop performance maps that predict isentropic efficiency over a wide range of working conditions. Additionally, cost correlations are established to predict price as a function of nominal compressor inlet volumetric flowrate. When rotary-vane compressors are an available option (i.e., for inlet volumetric flowrates up to $5 \bullet 10^{-3}$ m^3/s), they consistently achieve a high isentropic efficiency (~70 %) for the investigated pressure ratios (1.5–9.5). Scroll compressors have an even higher isentropic efficiency (~75 %) at pressure ratios below 5.5, but this drops to 50 % at higher pressure ratios, while the isentropic efficiency of reciprocating-piston compressors is best (~75 %) at higher pressure ratios (5.5–7.5). Utilising an air-source heat pump model, the compressor types are compared for countries with different weather characteristics and electricity prices. Rotary-vane compressors are associated with the lowest levelised cost of heat, but the comparison largely depends on location and heating requirements.

1. Introduction

The provision of space heating, space cooling and hot water in an efficient and low-carbon way is crucial to meet sustainability goals in every part of the world [1]. Heating and cooling account for more than half of the total energy consumption globally and almost 20 % of global emissions are attributed to the residential sector [2]. Several major economies have yet to decarbonise heating in buildings, and, as recently stated by the International Renewable Energy Agency, progress worldwide is still inadequate [3]. For example, 69 % of domestic heating in the US still relies on natural gas [4], and 86 % of UK homes still utilise gas boilers for heating [5].

One of the main low-carbon alternatives to gas and oil boilers are electric heat pumps. Heat pumps only need a fraction of the energy required by traditional boilers [6]. One of their main drawbacks has been that in many countries, the electricity prices are significantly high compared to natural gas prices [7], making them less cost-effective than traditional gas-driven options. However, their high thermodynamic performance together with the increasing pressure for heat decarbonisation [8] and the integration of more and more renewable energy sources on the electricity grid [9] make electric heat pumps one of the most promising technologies to meet global sustainability goals.

Electric heat pumps in domestic and commercial heating applications use electricity to transfer heat from a cold source to hot water [10]. The coefficient of performance (COP), which is the total heat provided over the electricity consumed, is the most commonly used metric to evaluate heat pump performance [11]. The COP and cost of heat pumps depend on various design variables, including the choice of heat source (air, ground, water), type or size of components (compressors, expansion valves, heat exchangers), and working fluid selection.

A core component of electric heat pumps is the compressor. The selection and sizing of the compressor depends on the operating conditions (e.g., evaporating and condensing pressures and temperatures), working fluid type and mass flowrate, space requirements and noise [12–14]. The compressor plays a vital role in the system's design and off-design operation.

This study specifically focuses on three primary compressor types:

* Corresponding author.
E-mail address: c.markides@imperial.ac.uk (C.N. Markides).

https://doi.org/10.1016/j.energy.2023.130171
Received 25 April 2023; Received in revised form 24 December 2023; Accepted 27 December 2023
Available online 28 December 2023
0360-5442/© 2023 The Authors. Published by Elsevier Ltd. This is an open access article under the CC BY license (http://creativecommons.org/licenses/by/4.0/).

Nomenclature

Abbreviations

ASHP	air-source heat pump
COP	coefficient of performance
GWP	global warming potential
LCOH	levelised cost of heat
PBT	payback time
RMSE	root-mean square error

Symbols

α_1 to α_6	polynomial coefficients
C	cost [£]
c_1 and c_2	regression coefficients
d	discount rate [−]
h	specific enthalpy [J/kg]
η	efficiency [−]
i	inflation rate [−]
$\dot{m}$	mass flowrate [kg/s]
M_1 to M_{10}	regression coefficients
n	heat pump lifetime [years]
L_1 to L_{10}	regression coefficients
Q	heat production [J]
$\dot{Q}$	heating rate [W]
r_P	pressure ratio [−]
T	temperature [°C,K]
$\dot{V}$	volumetric flowrate [m^3/s]
$\dot{W}$	power input [W]

Subscripts/superscripts

ann	annual
comp	compressor
d	discharge
in	inlet
inv	investment
is	isentropic
op	operation
out	outlet
s	suction
sav	savings
sink	heat sink
src	heat source
wf	working fluid

rotary-vane, scroll, and reciprocating-piston, based on their prevalence in domestic applications, as highlighted in a recent analysis conducted by the authors of the UK heat pump market [15].

1.1. Overview of small-scale heat pump compressor types

Positive displacement compressors, distinguished by their operation at lower speeds in comparison to dynamic compressors, can generally achieve significantly higher compression ratios and they are found in all commercially available small-to medium-sized (15 kW_{th}) vapour-compression heat pump systems. They rely on capturing a volume of fluid and reducing it to increase the fluid pressure, and can be categorised into rotary machines, such as the rotary-vane and scroll compressors, and reciprocating machines, such as the reciprocating-piston compressors.

Rotary-vane compressors are the most common compressor type on the domestic heat pump market [16]. They are composed of cylindrical cases housing a rotor positioned eccentrically, featuring vane slots. As the rotor revolves, the vanes slide out to touch the chamber walls, trapping the working fluid. Consequently, the volume housing the fluid is gradually reduced during rotation, leading to the compression of the working fluid. Noteworthy advantages of rotary-vane compressors encompass their compactness, low weight, and cost-effectiveness [17,18]. A key limitation arises from friction between components, potentially impacting efficiency under high pressures and shortening their operational lifespan. Current research emphasis revolves around minimising friction losses, particularly at the tips of the sliding vanes, which were identified as the primary contributor to frictional losses [19]. Various models, ranging from 1-D types [19] to more complex 3-D models [20–22], have been proposed to capture the characteristics of these losses. Bianchi and Cipollone [23] have suggested potential methods for reducing friction losses, such as employing low revolution speeds and utilising lighter vane materials.

Scroll compressors are also found in several commercially available heat pumps. They often use two intermeshing scrolls to pressurise working fluids where one scroll is fixed and the other orbits eccentrically without rotating. When the orbiting scroll moves, there is a decrease in the space between the two scrolls which results in the compression of the working fluid. Due to their design, scroll compressors possess few moving parts, resulting in low vibration, which in turn leads to reduced noise and extended operational lifespans [24,25]. Several experimental and theoretical assessments have been performed to assess different configurations of scroll compressors across various working fluid types [26–28]. Scroll compressors were shown to exhibit superior performance at lower pressure ratios (i.e., between 3 and 5). However, their efficiency reduces exponentially beyond a specific pressure ratio, typically ranging between 5 and 7, a value that varies among different designs and manufacturers [29,30].

Reciprocating-piston compressors operate based on a crankshaft which converts rotary motion into reciprocating movement, which translates to a piston that compresses the working fluid by pushing it into an enclosed cylindrical space. Their efficiency is influenced by the number of valves, cylinders, bodies, and compression stages [31]. These compressors are recognised for their ability to handle high pressures and maintain robustness across different operational loads [32,33]. Ongoing research predominantly targets the enhancement of the efficiency by optimising specific design parameters such as the cylinder-piston gap, clearance volume and valve thickness [34]. Furthermore, a crucial area of focus involves minimising losses attributed to piston rings [35], as well as losses (both steady and unsteady/exergy) due to heat transfer [36–38].

1.2. Research gap and novelty of this work

When optimising the design and operation of small-scale heat-pumping and other energy-conversion systems, an understanding of the performance of different compressor types at various operating conditions is necessary. Technology modellers commonly rely on existing compressor efficiency maps to predict performance under specific working conditions [32,39,40]. These maps are typically derived from experimental investigations [41], manufacturer data [42] or detailed thermodynamic models [33,43]. For example, Wang et al. [32] used a data-driven screw compressor performance map proposed by Astolfi et al. [42], the experimental data for scroll expanders from Lemort et al. [41] and a comprehensive model of a reciprocating-piston expander by Simpson et al. [33,43] to perform a comprehensive assessment of solar organic Rankine cycle (ORC) systems. Furthermore, Lemort et al. [44] compared expander types based on empirical (black-box) and semi-empirical (grey-box) models [28,32] in the literature (e.g., Refs. [41,45]). However, comparing compressors based on performance maps

obtained through different methodologies poses a challenge, as they are developed using varying assumptions, sizes, and working fluids. Consequently, a literature gap exists in the establishment of comprehensive and consistent methods for estimating both compressor performance and cost, hindering a like-to-like comparison of different compressor types.

This paper addresses the aforementioned literature gap by introducing two novel contributions:

1. Uniform modelling approach: For the first time, we use a consistent, like-to-like modelling approach to develop reliable and simple-to-use performance maps and cost correlations for rotary-vane, scroll and reciprocating-piston compressors targeted for small-scale applications. The performance maps, which are developed through an analysis of information gathered for 120 commercial compressors (40 for each type), enable the prediction of isentropic efficiency as a function of compressor operating pressure ratio and inlet volumetric flowrate, and their applicability spans a wide range of operating conditions. The cost correlations enable the prediction of compressor price as a function of inlet volumetric flowrate.
2. Technoeconomic comparison: Utilising the established cost and performance maps, we conduct a technoeconomic comparison of heat pumps using rotary-vane, scroll, and reciprocating-piston compressors. This analysis is used to, for the first time, identify the conditions under which each compressor type proves competitive. It encompasses various heat pump sizes and considers diverse geographical locations with distinct weather patterns and electricity price characteristics.

By adopting a consistent modelling approach and conducting a detailed technoeconomic comparison, this paper contributes to a meaningful evaluation of different compressor types for small-scale heat-pumping applications. In Section 2, the development of the compressor database, the associated performance maps and the heat pump case study are described. In Section 3, the cost and performance maps are presented and the different heat pump designs are technoeconomically compared. Concluding remarks are provided in Section 4.

2. Methodology

In this section, the methodology for the development of compressor performance maps and cost correlations is explained. Then, the heat pump case study is presented.

The heat pump cycle, which in its simplest form involves a condenser, an evaporator, an expansion valve and a compressor, is shown in Fig. 1. The three main compressor types found in commercially available domestic heat pumps are rotary-vane, scroll and reciprocating-piston compressors [15].

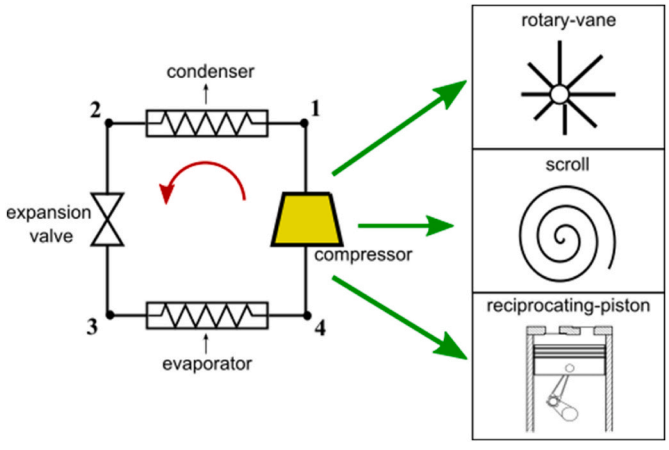


Fig. 1. Heat pump cycle and main compressor types used in domestic heat pumps.

2.1. Isentropic efficiency estimation

Compressor performance is often reported by manufacturers using the ten-coefficient polynomial method suggested by the Air-Conditioning, Heating Refrigeration Institute [46]. Although this method involves a black-box model and does not account for the properties of different working fluids or the physical characteristics related to the compression method [47], it is a convenient and widely used method to predict compressor performance based on the suction dew point temperature T_s (equal to that of a heat pump condensation temperature) and the compressor discharge temperature T_d (equal to that of a heat pump evaporation temperature). Using the aforementioned conditions and the ten-coefficient polynomials shown in Equations (1) and (2), the mass flowrate of the working fluid, $\dot{m}_{wf}$, and the power input required by the compressor, $\dot{W}_{comp}$, can be predicted:

$$\dot{m}_{wf} = M_1 + M_2 T_s + M_3 T_d + M_4 {T_s}^2 + M_5 T_s T_d + M_6 {T_d}^2 + M_7 {T_s}^3 + M_8 {T_s}^2 T_d + M_9 T_s {T_d}^2 + M_{10} {T_d}^3, \quad (1)$$

$$\dot{W}_{comp} = L_1 + L_2 T_s + L_3 T_d + L_4 {T_s}^2 + L_5 T_s T_d + L_6 {T_d}^2 + L_7 {T_s}^3 + L_8 {T_s}^2 T_d + L_9 T_s {T_d}^2 + L_{10} {T_d}^3, \quad (2)$$

where M_1 to M_{10} and L_1 to L_{10} are the regression coefficients provided for each compressor by manufacturers.

A database of compressor polynomial regression coefficients is created, which includes regression coefficient data for 40 compressors for each examined type. These were selected to have volumetric flowrates up to $15 \bullet 10^{-3}$ m^3/s. The flowrate constraint corresponds to small-scale heat pump applications (<30 kW_{th} for most working fluids and heat-source temperatures between −15 °C and 20 °C). Data from several manufacturers were used: Bitzer [48], Panasonic, GCC, Bristol, Kulthorn and AVIC [49]. All obtained coefficients have been provided in the Supplemental Information document.

The fluid thermophysical equilibrium and transport properties, such as density and enthalpy, are evaluated at both the inlet and outlet of every compressor for a wide spectrum of operating conditions encompassing air temperatures ranging from −15 °C to 20 °C and hot-water delivery temperatures ranging from 30 °C to 60 °C. Numerous equations of state are available to calculate these properties, but the most applied method is the use of REFPROP [50], a computer software developed by the U.S. National Institute of Standards and Technology. REFPROP involves the use of validated mathematical models to provide these properties for a variety of industrially useful fluids and fluid mixtures, and it has been often used by industry, government, and academia. REFPROP is accessed through its graphical-user-interface in the MATLAB programming environment [51].

The selection of the aforementioned temperature ranges, which fall within the valid intervals for the provided polynomial models, is based on three primary considerations. First, they are chosen to cover the typical operational temperature ranges of domestic heat pumps, aligning with the operating specifications of popular models such as the Mitsubishi Ecodan [52] and Panasonic Aquarea [53] heat pumps. Second, these ranges span a broad spectrum of air temperatures, allowing for an examination of heat pump performance in various geographic locations with diverse climate characteristics [54]. Third, the chosen ranges cover a wide array of hot-water temperatures, ranging from applications such as domestic hot water, which necessitates temperatures of around 55–60 °C for legionella control [55], to underfloor heating applications where temperatures may be as low as 30–45 °C [56,57].

The isentropic efficiency is defined as the work that would be required in an isentropic compression process, $\dot{W}_{comp,is}$, over the work that is actually required, $\dot{W}_{comp}$. By employing the compressor ten-coefficient polynomials presented in Equations (1) and (2), $\dot{m}_{wf}$ and $\dot{W}_{comp}$ are calculated for all air and hot-water temperature combinations. Using the latter parameters and the calculated enthalpies from REFPROP, the isentropic efficiency, $\eta_{comp,is}$, is determined for all compressors in the database across all investigated operating conditions using:

$$\eta_{comp,is} = \frac{\dot{W}_{comp,is}}{\dot{W}_{comp}}, \tag{3}$$

where:

$$\dot{W}_{comp,is} = \dot{m}_{wf}\left(h_{2,is} - h_1\right), \tag{4}$$

$$\dot{W}_{comp} = \dot{m}_{wf}(h_2 - h_1)\ . \tag{5}$$

In Equations (4) and (5), $h_{2,is}$ is the specific enthalpy of the working fluid at the compressor outlet assuming isentropic compression, h_2 is the actual specific enthalpy of the working fluid at the compressor outlet and h_1 is the specific enthalpy of the working fluid at the compressor inlet. An electrical motor efficiency of 95 % is assumed [58].

2.2. Working fluids in compressor database

The collected compressor data is based on various working fluids, which are listed in Table 1. The working fluid selection has a significant effect on the operation of a compression device. Compressors are often manufactured to perform best when operated with a specific working fluid, which means that the performance with other fluids might deteriorate. It is also important to mention that legislation regarding the use of different working fluids in heat-pumping and refrigeration applications has become stricter [59,60] due to the significant negative impact that some of them can cause to the environment in the event of leakage. The global warming potential (GWP) is used as a measure of a fluid's contribution to global warming. The choice of working fluid thus requires finding a suitable balance between the objectives of high COP, low GWP and adequate safety.

The list of investigated working fluids is based on the availability of manufacturer data. R22 and R134a were common working fluids in the past, and several compressors are still designed for these fluids. However, they have been now phased out from domestic applications due to environmental concerns. In detail, R22 has a significantly high GWP of 1 960, while it also depletes the ozone, and R134a has a GWP of 1 530 [61]. R410A is currently one of the most used working fluids in domestic heat pumps [15], but it also has a very high GWP of 2 256. R32 appears in most newly designed heat pumps, as it shows a good performance and has a lower GWP (771). R407C is a blend of R32, R134a and R125. Lastly, hydrocarbon-based (e.g., propane) compression machines also appear on the market. Hydrocarbons are natural working fluids with negligible GWP compared to the aforementioned hydrochlorofluorocarbons (R22) and hydrofluorocarbons (R134a, R410A, R407C, R32) and can potentially dominate the market in the near future [62].

Table 1
Working fluids in the compressor database.

Compressor type	Working fluid
Rotary-vane	R134a, R410A, R407C, R32, propane
Scroll	R22, R134a, R410A, R407C, R32
Reciprocating-piston	R134a, R407C, R32

2.3. Compressor performance maps and cost correlations

Based on the collected data and the calculated isentropic efficiencies, performance maps have been generated to represent the isentropic efficiency as a function of volumetric flowrate at the compressor inlet, $\dot{V}_{comp,in}$, and compressor pressure ratio r_p. The pressure ratio, which is also often referred to as the compression ratio, is defined as the ratio of the condenser pressure to the evaporator pressure. These maps are constructed through second-order polynomial fits using the least-squares method, and they take the form of:

$$\eta_{comp,is} = \alpha_1 + \alpha_2 r_p + \alpha_3 \dot{V}_{comp,in} + \alpha_4 {r_p}^2 + \alpha_5 r_p \dot{V}_{comp,in} + \alpha_6 {\dot{V}_{comp,in}}^2, \tag{6}$$

where α_1 to α_6 represent the obtained polynomial coefficients.

The developed compressor performance maps represent the average performance of commercially available compressors. These maps can be used to estimate compressor performance with reasonable accuracy and are simple enough to be easily used by technology modellers when optimising heat-pumping and power-generation systems with compressors or expanders.

Since the collected data involves different fluids, generating a different map for each fluid would enhance the model accuracy, but this would be impractical for modellers performing design exercises with other fluids than those presented in Table 1. Therefore, the performance of compressors with different fluids is averaged, and the associated root-mean square error (RMSE) is provided with each map.

In order to technoeconomically compare different compressor types, information regarding the price of such machines is also required. Detailed datasets for each compressor type [15] are used to generate cost correlations to predict compressor cost as a function of compressor inlet volumetric flowrate. The correlations are power-regression models (as these have shown lower RMSEs than linear-regression or exponential regression models) and take the form:

$$C_{comp} = c_1 {\dot{V}_{comp,in}}^{c_2}, \tag{7}$$

where C_{comp} is the compressor cost, and c_1 and c_2 are the obtained regression coefficients.

2.4. Heat pump case studies

The thermodynamic and component-costing heat pump model developed in previous work of the authors [16] is used here to compare how different compressors affect the cost and performance of small-scale heat pumps. The heat pump model is spatially lumped and assumes negligible pressure loss across pipes and steady-state operation of components. The heat pump cycle processes, with reference to Fig. 1, are the following: working fluid compression (Process 1–2); heat rejection from working fluid to heat-sink fluid (Process 2–3); isenthalpic expansion through the expansion valve (Process 3–4); and heat addition from heat-source fluid to working fluid (Process 4-1). The main equations of the cycle and the component cost correlations are provided in Appendices A and B, respectively.

Two modelling exercises are performed in Sections 3.2 and 3.3. In the first exercise, optimal heat pump designs are obtained for two different air temperatures (7 °C and −15 °C) and three different heat pump sizes (nominal heat outputs of 10 kW_{th}, 20 kW_{th} and 30 kW_{th}). The temperature of 7 °C corresponds to the standard conditions for which heat pump performance is reported by manufacturers [63], and the temperature of −15 °C is used to assess performance in significantly colder locations. The competitiveness of the investigated compressor types is assessed for each of these scenarios. Then, the second modelling exercise involves performing an annual analysis and a calculation of the levelised cost of heat (LCOH) and payback time (PBT) associated with heat pumps based on each of the three compressor types.

The first modelling exercise involves the use of a heat pump design

optimisation problem. In this process, the heat pump cycle parameters are optimised with the objective to maximise the COP. A pinch-point temperature difference of 5 °C is assumed in all heat exchangers and the hot-water demand temperature is fixed at 55 °C. The decision variables of the optimisation problem involve the evaporation pressure, the condensation pressure, the degree of superheating and the degree of subcooling. The degree of superheating is constrained to be at least 5 °C to ensure that no liquid refrigerant enters the compressor. Once the optimal heat pump cycle is obtained, the heat exchangers and compressor are sized, and the validated cost correlations are used to estimate the cost of different heat pump components. In this work, the heat pump thermodynamic and component-costing model has been adapted to use the newly developed performance maps and cost correlations. Detailed information on the heat exchanger modelling methodology can be found in our previous work [16].

In the second modelling exercise, an off-design heat pump operation optimisation problem is also solved. Following the design exercise, for each set of operating conditions, the heat pump cycle is optimised for maximum COP while keeping component sizes fixed. This optimisation problem involves two decision variables: (i) the degree of superheating, which is assumed to be controlled using an electronic expansion valve; and (ii) the working fluid mass flow rate, which is modulated by a variable-speed compressor [64]. The analysis has been performed for three geographical locations with different weather characteristics: the UK, which represents a location with mild summers and winters; Finland, which is significantly colder than the UK in winter; and Greece, which has much warmer winters than the other two locations.

The LCOH and the PBT are defined, respectively, as follows [65,66]:

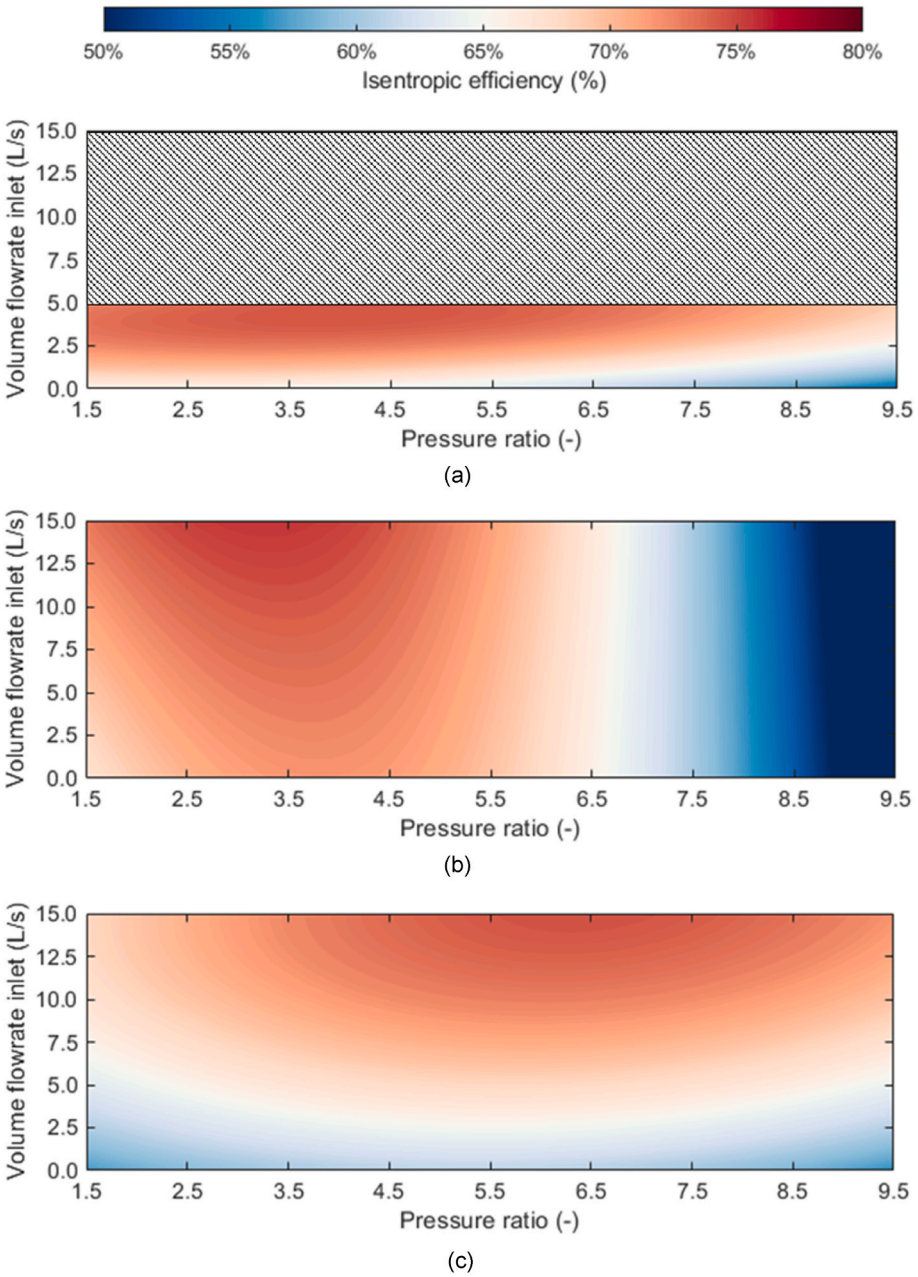


Fig. 2. Compressor performance maps for three compressor types: (a) rotary-vane; (b) scroll; and (c) reciprocating-piston. The maps show the isentropic efficiency as a function of compressor inlet volumetric flowrate and pressure ratio. They are obtained based on the performance curves of 120 commercially available compressors. The map for rotary-vane compressors is constrained to volume flowrates lower than $5 \bullet 10^{-3}$ m^3/s due to unavailability of data for higher flowrates.

$$C_{\mathrm{LCOH}} = \frac{C_{\mathrm{inv}} + \sum_{k=1}^{n} C_{\mathrm{op,ann}}(1+r)^{-k}}{\sum_{k=1}^{n} Q_{\mathrm{ann}}(1+r)^{-k}} \tag{8}$$

$$t_{\mathrm{PBT}} = \frac{\ln\left[\frac{C_{\mathrm{sav,ann}}}{C_{\mathrm{sav,ann}} - rC_{\mathrm{inv}}}\right]}{\ln[1+r]} \tag{9}$$

where C_{inv} is the investment cost (heat pump price and installation), $C_{\mathrm{op,ann}}$ the annual operational and maintenance cost, r the real discount rate, Q_{ann} the annual heat production, n the heat pump lifetime and $C_{\mathrm{sav,ann}}$ the annual cost savings. For this analysis, a heat pump lifetime of 20 years, an installation cost of £2 300 [67] and an annual maintenance cost of £100 [68] are assumed. The real discount rate is set to 3 % [69]. The annual cost savings represent the difference in operational cost when the heat demand is met by an electric heat pump compared to an electric boiler.

3. Results and discussion

In this section, the compressor maps and cost correlations obtained from the data collection and regression analysis are first presented and discussed. Then, the compressors are compared for different heat pump design conditions (sizes and weather characteristics). Finally, the annual technoeconomic performance analysis of different heat pumps for three geographical locations with different weather characteristics are presented.

3.1. Compressor performance maps and cost correlations

The compressor performance maps obtained in this work and the polynomial coefficients corresponding to Equation (6) are presented in Fig. 2 and Table 2, respectively. The RMSE and R^2 values associated with each map are also provided in Table 2. Furthermore, the developed cost correlations and relevant RMSE and R^2 values are provided in Fig. 3.

Some interesting observations can be made from Fig. 2. Rotary-vane compressors achieve high performance (isentropic efficiency between 65 % and 75 %) for the whole range of pressure ratios (1.5–9.5) except if the compressor inlet volumetric flowrate is below $2 \bullet 10^{-3}$ m^3/s and the pressure ratio is higher than 6.5. However, rotary-vane compressors available on the market are associated with volumetric flowrates lower than scroll and reciprocating-piston compressors and therefore the map is not extended to flowrates higher than $5 \bullet 10^{-3}$ m^3/s.

Scroll compressors achieve a high isentropic efficiency (>70 %) for pressure ratios below 5.5. This is true for all investigated volumetric flowrates. The maximum isentropic efficiency for scroll compressors (77 %) is obtained at a pressure ratio between 2.5 and 4.5 and a volumetric flowrate between $11 \bullet 10^{-3}$ and $15 \bullet 10^{-3}$ m^3/s. This means that scroll compressors are well suited for heat-pumping applications with relatively small temperature differences between the heat-source and -sink fluids (as the smaller the temperature difference, the smaller the compressor pressure ratio). However, there is an abrupt change for pressure ratios higher than 5.5, with the isentropic efficiency significantly reducing to ~50 % for pressure ratios higher than 8.5.

Unlike scroll compressors, reciprocating-piston compressors show a better performance at high pressure ratios. The isentropic efficiency is best (>70 %) for pressure ratios between 5.5 and 7.5 and volume flowrates above $2.5 \bullet 10^{-3}$ m^3/s, but it drops below 65 % for volume flowrates lower than $2 \bullet 10^{-3}$ m^3/s. The maximum isentropic efficiency is 76 %, but this is obtained at a pressure ratio between 5.5 and 6.5 and a volumetric flowrate between $13 \bullet 10^{-3}$ and $15 \bullet 10^{-3}$ m^3/s.

As demonstrated in Fig. 3, rotary-vane compressors for which cost information is available have lower volumetric flowrates than scroll and reciprocating-piston compressors. It is evident that rotary-vane compressors are targeted for smaller-scale applications than the other two types. Furthermore, rotary-vane compressors are generally cheap, costing less than £1 000 for the considered sizes. For volumetric flowrates up to $20 \bullet 10^{-3}$ m^3/s, scroll and reciprocating-piston compressor costs vary between £100 and £10 000. Scroll compressors are often shown to be slightly more expensive than reciprocating-piston compressors but this depends on the choice of design and manufacturer.

It is important to note that the number of compressors being ordered is not captured in the relationships shown in these figures. Heat pump manufacturers may place bulk orders for compressors, potentially impacting unit price. However, it is anticipated that the number of compressors purchased would have a comparable impact on the costs of all three compressor types. As a result, this factor does not significantly affect the compressor technoeconomic comparisons of the next sections.

3.2. Comparison of compressors at different design conditions

In this section, optimal heat pump designs are obtained for three ASHP sizes (nominal heat outputs of 10 kW_{th}, 20 kW_{th} and 30 kW_{th}) and two air temperatures (7 °C and −15 °C). All designs are optimised for a hot-water delivery temperature of 55 °C. The working fluid is chosen to be R32, as this is one of the most common domestic heat pump fluids in recent years. First, the heat pump COP is plotted as a function of outside air temperature for each of three compressor types based on the performance maps and cost correlations derived in this paper (Fig. 4). Then, the component-cost breakdown and nominal COP of the optimal designs for the three heat pump sizes are presented (Fig. 5).

As shown in Fig. 4, scroll compressors achieve a lower COP than rotary-vane and reciprocating-piston compressors at low air temperatures (<−2 °C). However, their COP is higher than both other types at high air temperatures (>5 °C). Rotary-vane compressors, on the other hand, are the best option from a technical perspective for temperatures below 2 °C, while their COP at high temperatures (>5 °C) is slightly lower than scroll but much higher than reciprocating-piston compressors.

Furthermore, it is evident from Fig. 5 that heat pumps designed based on rotary-vane compressors are associated with the lowest investment costs in all scenarios. However, using the developed compressor performance maps and cost correlations, 30 kW_{th} heat pumps can only be based on scroll or reciprocating-piston compressors, due to the size restrictions associated with rotary-vane compressors.

When heat pumps are designed for an air temperature of 7 °C, those based on rotary-vane and scroll compressors achieve a higher COP than those based on reciprocating-piston compressors. For both rotary-vane and scroll compressors, a nominal COP of ~3 is obtained for the considered sizes. Although the performance is similar, heat pumps involving scroll compressors are significantly more expensive than those based on rotary-vane ones (difference varies between £1 000−£2 000 for different sizes). Reciprocating-piston compressors are shown to be slightly cheaper than scroll compressors by £300−£500 but the COP is

Table 2
Polynomial coefficients for the calculation of isentropic efficiency for each compressor type and associated RMSE and R^2 values. The coefficients correspond to those in Equation (6).

Compressor type	α_1	α_2	α_3	α_4	α_5	α_6	RMSE	R^2
rotary-vane	0.644	0.00910	38.8	−0.00210	1.87	−5410	1.43 %	0.96
scroll	0.593	0.0660	4.89	−0.00860	−0.654	0.00	1.46 %	0.98
reciprocating-piston	0.533	0.0290	15.1	−0.00270	0.359	−545	1.34 %	0.97

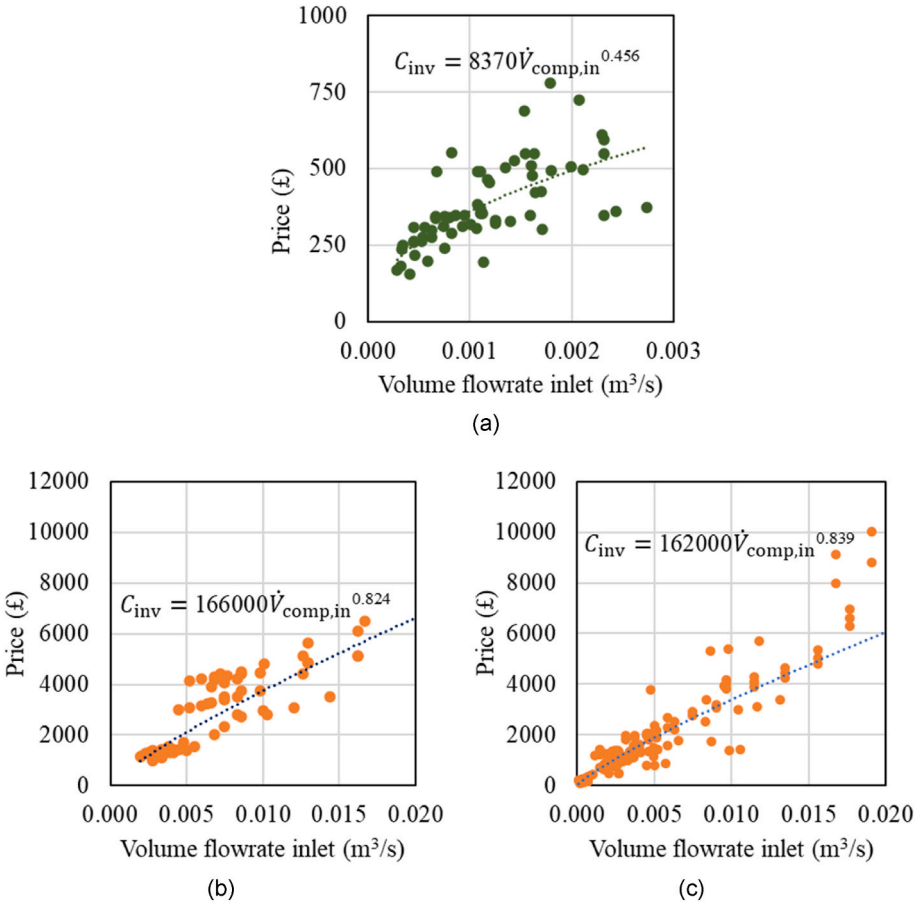


Fig. 3. Compressor price as a function of volumetric flowrate at compressor inlet for three types of compressors: (a) rotary-vane; (b) scroll; and (c) reciprocating-piston. The RMSEs associated with these correlations for the prices of rotary-vane, scroll and reciprocating-piston compressors are equal to £100, £817 and £818, respectively, and the R^2 values are equal to 0.47, 0.84 and 0.95, respectively.

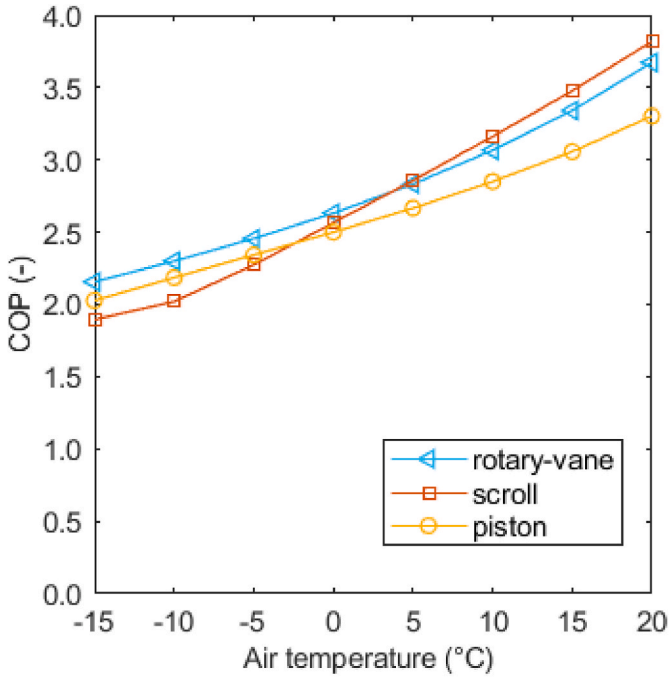


Fig. 4. Heat pump COP as a function of outside air temperature for each of the three compressor types (rotary-vane, scroll, reciprocating-piston). The hot-water delivery temperature is fixed at 55 °C.

up to 10 % lower.

The comparison changes when examining heat pumps designed for colder regions, particularly those designed for an air temperature of −15 °C. In cases where rotary-vane compressors are an available option (for the 10 kW_{th} and 20 kW_{th} heat pumps), the heat pumps based on these compressors are associated with the lowest cost and best performance (nominal COP close to 2.2). The significantly higher pressure ratio, arising from the large temperature difference between the heat-source and -sink fluids, results in a significant deterioration in the performance of scroll compressors, which achieve the lowest COP (~1.8) at this temperature. Conversely, reciprocating-piston compressors perform well under high pressure ratios, consistently achieving a COP higher than 2 across all considered sizes. Especially for the 30 kW_{th} case, reciprocating-piston compressors are shown to achieve a COP that is 13 % higher than scroll compressors and this enhanced performance is achieved without notable additional cost.

3.3. Levelised cost of heat and payback time for different locations and applications

In this section, results from an annual performance analysis of three heat pump designs based on rotary-vane, scroll and piston compressors are presented. The analysis is performed for three geographical locations with different weather characteristics. The selection of these locations was guided by an examination of temperature profiles sourced from the datasets of Sansom [70] and Ruhnau et al. [71], encompassing 28 European countries. Three countries are chosen to ensure a comprehensive representation of varied weather conditions across Europe. The UK is selected to represent a location with mild summers and winters, Finland

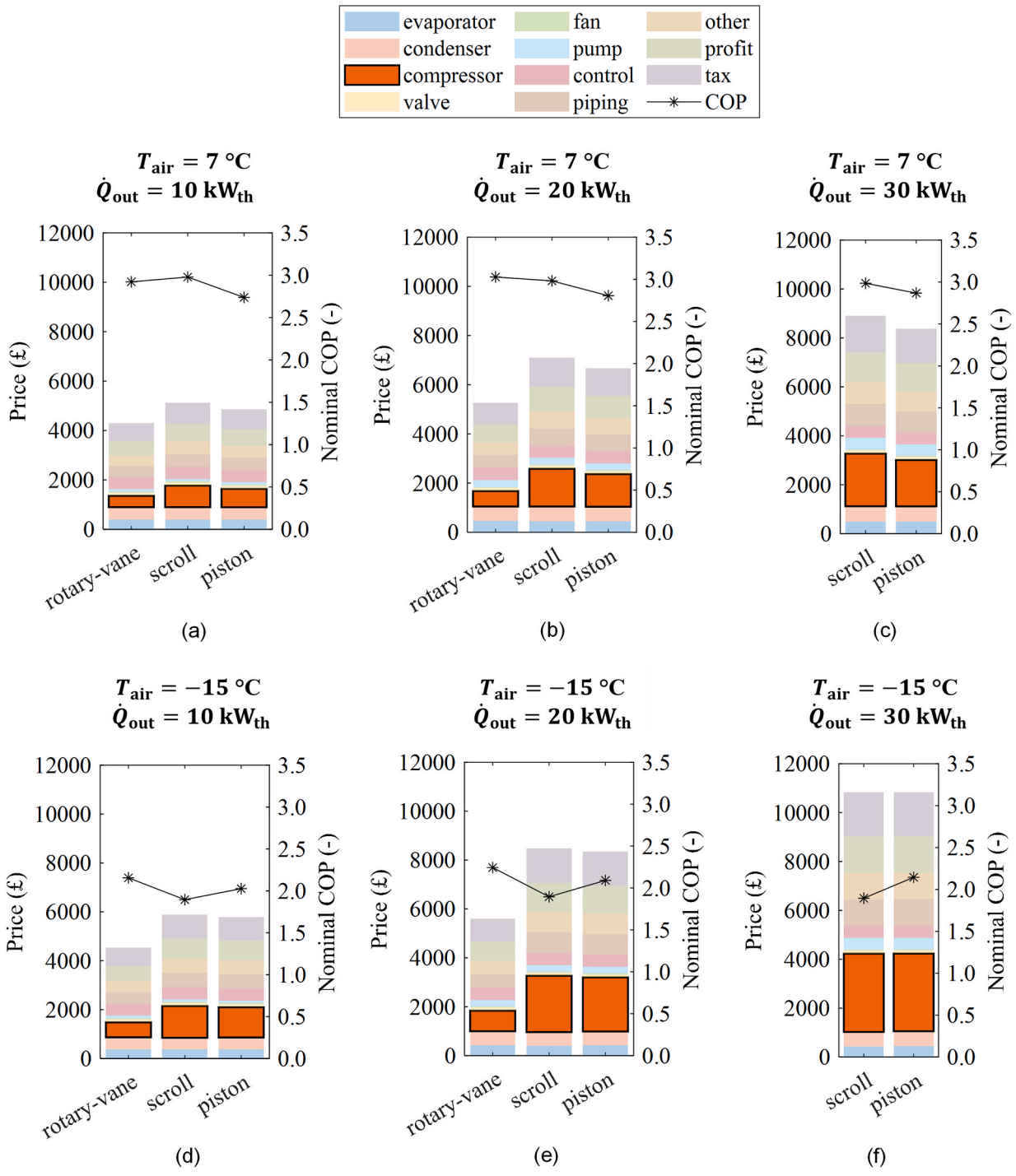


Fig. 5. Heat pump component cost breakdown and nominal COP for six different design conditions. These include three sizes (nominal heat outputs of 10 kW_{th}, 20 kW_{th} and 30 kW_{th}) and two different air temperatures (7 °C and −15 °C). The nominal COP is calculated for a hot-water delivery temperature of 55 °C. The nominal heat output $\dot{Q}_{out}$ and air temperature T_{air} are provided at the top of each design.

to illustrate a notably colder winter climate, and Greece to exemplify much warmer winters than the other two regions. For each location, the comparison is conducted based on two heat demand profiles representing two different applications: an average household; and a commercial building with a peak heat demand of 30 kW_{th}. The hourly heat demand and temperature profiles are obtained from the work of Sansom [70] (based on the "cold" temperature profile) for the UK and Ruhnau et al. [71] for residential and commercial buildings in Finland and Greece.

Whenever there is demand, heat is assumed to be drawn from a hot-water cylinder and at the same time the heat pump is used to retain the temperature of the latter at 55 °C. Thus, the heat pump is sized based on the peak heat demand of the considered building. For the residential building case studies, the average household in each location has a different peak heat demand. A peak coincident factor (ratio of national peak heat demand over sum of peak loads of individual buildings) of 50 % is used to size the heat pumps, in line with estimates in Refs. [70,72]. This results in a heat pump size of 7 kW_{th} in the UK, 13 kW_{th} in Finland

and 5 kW_{th} in Greece. For the commercial building case studies, the heat pump is sized to equal the considered peak demand (30 kW_{th}) for all locations. For the calculation of LCOH and PBT, the domestic electricity price is fixed at 0.34 £/kWh for the UK [73], 0.37 £/kWh for Finland [74] and 0.22 £/kWh for Greece [75], based on the most recent available data.

The LCOH and PBT associated with the heat pumps designed for an average-size household of each of the three countries are shown in Fig. 6. Based on the considered compressor type, the LCOH is shown to vary in the range of196 –210 £/MWh, 195–208 £/MWh and 165–176 £/MWh for the UK, Finland and Greece, respectively. Rotary-vane compressors, which are significantly cheaper than scroll and reciprocating-piston compressors, lead to the lowest heat pump LCOH in all locations. Scroll compressors, which are the highest-performance type in high temperatures (Fig. 4), achieve a lower LCOH than reciprocating-piston compressors in the UK and Greece, however the LCOH of reciprocating-piston compressors is lower in Finland, which has much colder winters. It is interesting to also observe that the LCOH for rotary-vane and scroll compressors in Greece is almost the same (165–166 £/MWh), showing that scroll compressors can be competitive with rotary-vane compressors in warmer climates.

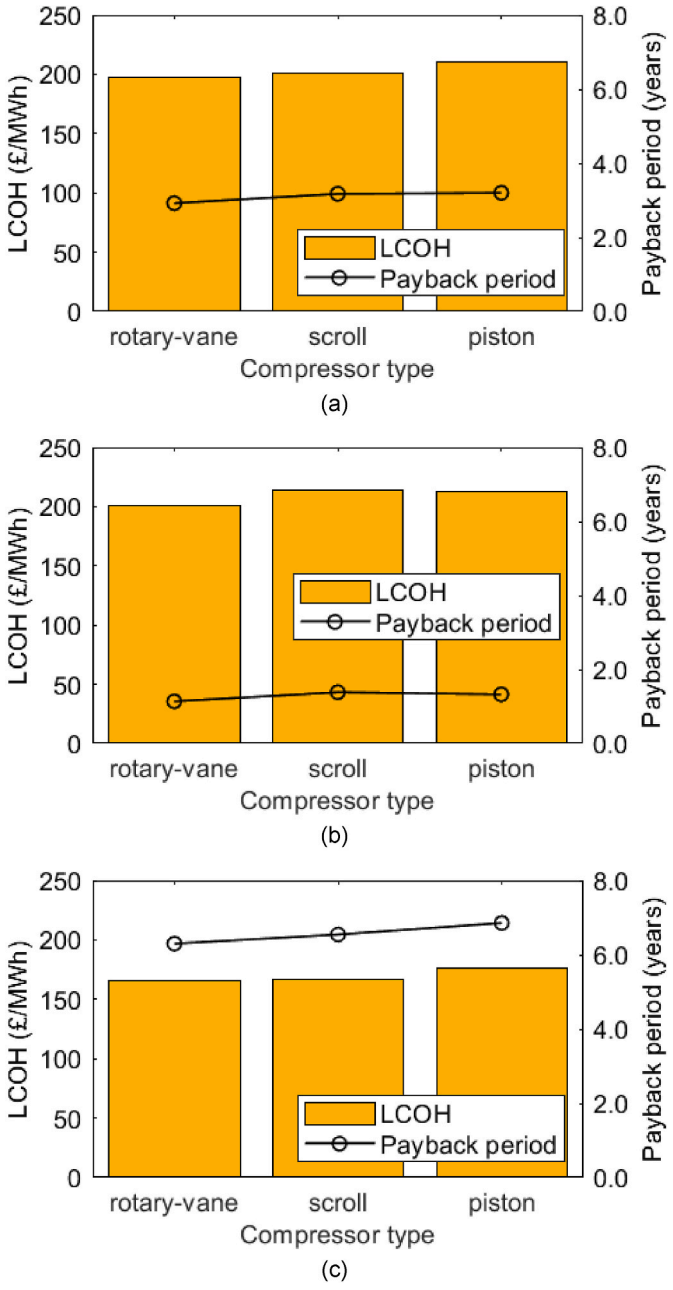


Fig. 6. LCOH and PBT for a heat pump sized to meet the heat demand of an average-size household based on rotary-vane, scroll and reciprocating-piston compressors for three locations with different weather characteristics: (a) UK; (b) Finland; and (c) Greece. The PBT represents the time it takes to recover the heat pump investment cost when switching from an electric boiler.

The PBT, which is the time required to recover the heat pump investment cost when switching from an existing electric boiler, depends significantly on the location. In the UK, the PBT varies between 3 and 4 years for all compressor types. In Finland, where the demand is higher, it is below 2 years, demonstrating the significant economic savings that can be obtained during the operation of an electric heat pump compared to that of an electric boiler. Correspondingly, the PBT is higher in Greece (6–7 years) due to the lower heat demand. The use of rotary-vane compressors leads to the minimum PBT in all cases due to the lower investment cost. Overall, for a typical household and given the considered weather conditions of the three locations, rotary-vane compressors are shown to be the most cost-effective option. However, an analysis of different heat pump sizes, applications and locations with more extreme weather conditions could lead to different optimal compressor types.

The LCOH and PBT for a heat pump sized to meet the heat demand of a commercial building with a peak heat demand of 30 kW_{th} for the three locations are shown in Fig. 7. Off-the-shelf rotary-vane compressors are not an available option at this size and are thus not included in the comparison. In all simulated cases, the PBT is less than 2 years. This is attributed to the considerable reduction in the specific heat pump cost when used in commercial buildings, as opposed to residential ones. Additionally, the use of heat pumps in commercial buildings yields to substantially higher operational savings throughout the heat pump lifetime. The variations in payback times among the different countries are relatively minor, as they are all focused on a commercial building with the same peak heat demand. The LCOH of scroll compressors is lower than reciprocating-piston compressors in the UK (153 £/MWh compared to 163 £/MWh) and Greece (97 £/MWh compared to 106 £/MWh), however, as in the case of household applications, reciprocating-piston compressors perform slightly better than scroll compressors in Finland (199 £/MWh compared to 201 £/MWh).

It should be mentioned that the PBT when switching from an electric boiler to an electric heat pump is significantly different from the PBT that would be obtained when switching from a gas boiler. In fact, at the current electricity and gas prices in the UK, for example, an electric heat pump provides negligible operational cost savings compared to a gas boiler. However, recent legislation on gas boilers for domestic applications is moving in a direction where these might not be an available option in the near future, and therefore, they are not considered here for comparison.

4. Conclusions

The primary aim of this work was to develop data-driven compressor performance maps and cost correlations which can be used to compare different compressor types in small-scale (<30 kW_{th}) heat-pumping and other energy-conversion applications from both technical and economic perspectives. This involved developing a database comprising published information on 120 commercially available compressor products. The obtained maps and correlations were integrated within a thermodynamic and component-cost heat pump model and the potential of different compressor types was analysed for different weather conditions and heat pump sizes.

The compressor performance maps were shown to predict the isentropic efficiency for a range of compressor volumetric flowrates and pressure ratios with sufficient accuracy; specifically, the RMSE was found to be below 2 % for all maps. Rotary-vane compressors were shown to achieve an isentropic efficiency higher than 65 % for the

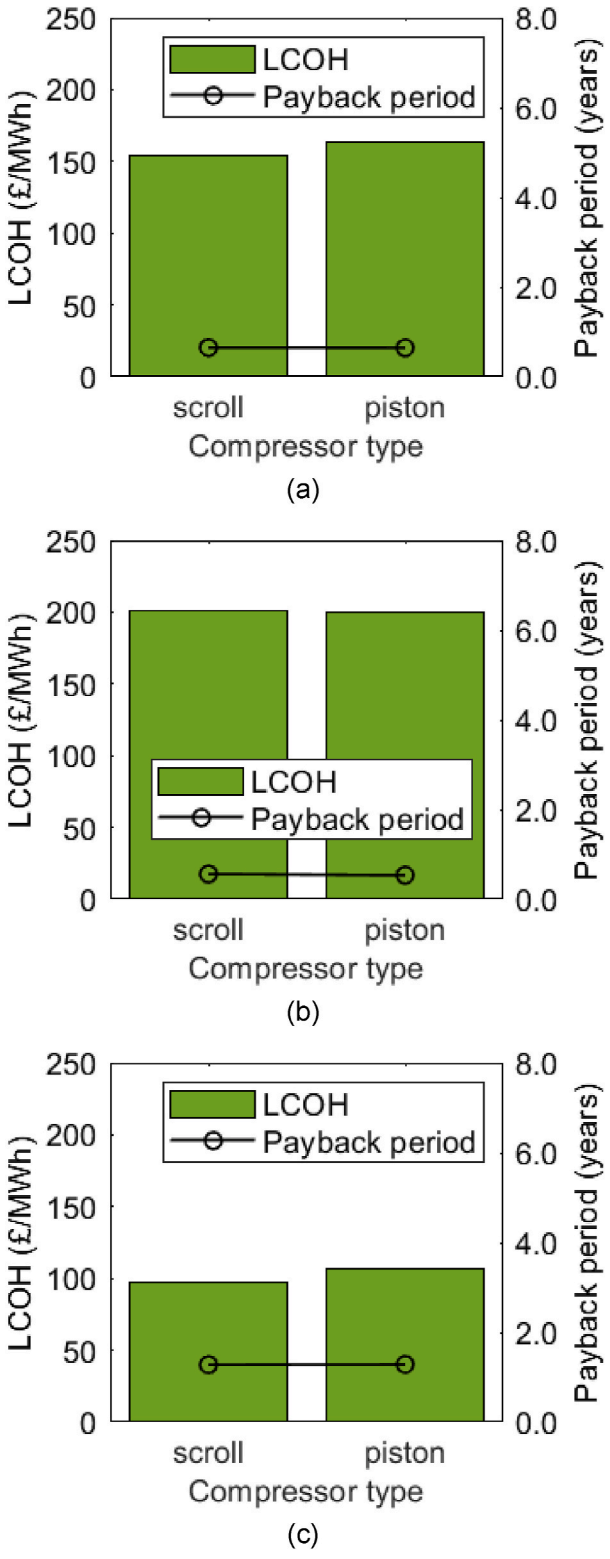


Fig. 7. LCOH and PBT for a heat pump sized to meet the heat demand of a commercial building with a peak heat demand of 30 kW_{th} based on scroll and reciprocating-piston compressors for three locations with different weather characteristics: (a) UK; (b) Finland; and (c) Greece. Rotary-vane compressors are not considered due to size restrictions. The PBT represents the time it takes to recover the heat pump investment cost when switching from an electric boiler.

investigated range of pressure ratios (1.5–9.5) but no commercially available units were identified for flowrates above $5 \bullet 10^{-3}$ m^3/s. Scroll compressors have an isentropic efficiency higher than 70 % for pressure ratios below 5.5, but the efficiency drops as low as 50 % for higher pressure ratios. Lastly, reciprocating-piston compressors perform best at high pressure ratios between 5.5 and 7.5 with an isentropic efficiency of over 70 %, but their performance is worse than rotary-vane and scroll compressors at lower pressure ratios.

Optimal heat pump designs were then obtained for three different heat pump sizes (nominal heat outputs of 10 kW_{th}, 20 kW_{th} and 30 kW_{th}) and two different air temperatures (7 °C and −15 °C). The techno-economic analysis showed that heat pumps based on rotary-vane compressors are cheaper than those based on scroll or reciprocating-piston compressors for all investigated conditions. The price of heat pumps based on rotary-vane compressors varied between £4 000 and £6 000 depending on the design point and size requirements. When heat pumps were designed for an air temperature of 7 °C, rotary-vane and scroll compressors led to a higher heat pump COP than reciprocating-piston compressors. In detail, the COP based on rotary-vane compressors was found to be close to 3 for a hot-water delivery temperature of 55 °C. However, when heat pumps were designed for an air temperature of −15 °C, reciprocating-piston compressors were more competitive than scroll compressors, as a COP beyond 10 % higher was achieved with similar costs.

Lastly, an annual performance comparison of heat pumps based on different compressor types was conducted for an average household and a commercial building in three locations with different weather characteristics:the UK, Finland and Greece. For the average household and based on each country's current electricity price for domestic consumers, heat pumps designed with rotary-vane compressors were shown to have the lowest LCOH (197 £/MWh in the UK, 200 £/MWh in Finland and 166 £/MWh in Greece) and lowest PBT when switching from an electric boiler (2.9 years in the UK, 1.1 years in Finland and 6.3 years in Greece). However, rotary-vane compressors are not a commercially available option at larger scales, and the competitiveness of scroll and reciprocating-piston compressors is affected by weather characteristics. For a commercial building with a peak heat demand of 30 kW_{th}, scroll compressors are more cost-effective than reciprocating-piston compressors in Greece, which has a warm climate, and in the UK, which has mild summers and winters, whereas reciprocating-piston compressors were shown to perform marginally better than scroll compressors in Finland, which has colder winters than the other locations.

It is noted that the conclusions of this work hold for these specific, small-scale applications and that the selection of the most suitable compressor for heat-pumping applications in general can also depend on other factors, including the specifics of the working fluid, heat demand profile, and heat pump control mechanism. Future work will focus on comparisons of LCOH and PBT for more locations, larger size ranges and more application examples in order to develop compressor selection maps that can identify the most cost-effective option over a wide range of operating conditions and control strategies in heat-pumping applications.

CRediT authorship contribution statement

Andreas V. Olympios: Conceptualization, Formal analysis, Methodology, Software, Writing – original draft, Writing – review & editing. **Jian Song:** Formal analysis, Methodology, Writing – original draft, Writing – review & editing. **Aleksander Ziolkowski:** Investigation, Software, Writing – original draft, Formal analysis. **Vethalingam S. Shanmugam:** Formal analysis, Software, Writing – original draft, Investigation. **Christos N. Markides:** Methodology, Project administration, Resources, Supervision, Writing – review & editing, Conceptualization.

Declaration of competing interest

The authors declare that they have no known competing financial interests or personal relationships that could have appeared to influence the work reported in this paper.

Data availability

Data will be made available on request.

Acknowledgments

This work was supported by the UK Engineering and Physical Sciences Research Council (EPSRC) [grant numbers EP/R045518/1, and EP/V042149/1] and UK Natural Environment Research Council (NERC) [grant number NE/L002515/1]. The authors would also like to acknowledge the Science and Solutions for a Changing Planet (SSCP) Doctoral Training Partnership (DTP). Data supporting this publication can be obtained on request from cep-lab@imperial.ac.uk. For the purpose of Open Access, the authors have applied a CC BY public copyright licence to any Author Accepted Manuscript version arising from this submission.

Appendix A. Heat pump cycle thermodynamic model

The main governing equations of the thermodynamic heat pump model are here presented. These are based on previous published work of the authors [16]. For a given set of working conditions within the examined ranges, the compressor performance maps developed in this specific work can be used to predict the compressor isentropic efficiency, $\eta_{is,comp}$. For a well-insulated compressor and given the specific enthalpy of the working fluid vapour at the compressor inlet is h_1, this isentropic efficiency can be used to estimate the working fluid specific enthalpy at the heat pump compressor outlet, h_2:

$$h_2 = h_1 + \frac{h_{2,is} - h_1}{\eta_{comp,is}}, \tag{A.1}$$

where $h_{2,is}$ is the specific enthalpy of a perfectly isentropic compressor. Equation (A.1) can be derived by solving Equations (3)–(5) of the main body of the manuscript. Given a working fluid mass flowrate, $\dot{m}_{wf}$, the compressor power input can be thus calculated:

$$\dot{W}_{comp} = \dot{m}_{wf}(h_2 - h_1)\ . \tag{A.2}$$

The compressed working fluid vapour then passes through the condenser, which is in this case a plate heat exchanger used to transfer heat from the working fluid to the desired heat-sink fluid. This process results in the condensation of the working fluid. The heat transfer rate at which heat is removed, which corresponds to the heat pump heat output, $\dot{Q}_{out}$, is equal to:

$$\dot{Q}_{out} = \dot{m}_{sink} c_{p,sink} \left(T_{sink,out} - T_{sink,in}\right), \tag{A.3}$$

where $\dot{m}_{sink}$, $c_{p,sink}$ and $T_{sink,out} - T_{sink,in}$ are the heat-sink fluid mass flowrate, its specific heat capacity its increase in temperature in the condenser, respectively. In the case of an air-to-water heat pump, the heat-sink fluid is hot water. The specific enthalpy of the working fluid during this process reduces to h_3 and the heat transfer rate, $\dot{Q}_{out}$, is equal to:

$$\dot{Q}_{out} = \dot{m}_{wf}(h_2 - h_3)\ . \tag{A.4}$$

The condensed working fluid then enters the expansion valve, where, for an isenthalpic flow-throttling process, the specific enthalpy at the valve output, h_4, is equal to:

$$h_4 = h_3\ . \tag{A.5}$$

The expanded working fluid lastly passes through the evaporator, which is here a plate fin heat exchanger corresponding to an air-to-water heat pump. The heat-source fluid from which heat is extracted is ambient air. In this process, the working fluid is evaporated and often superheated. The heat transfer rate from the heat-source fluid, $\dot{Q}_{in}$, is equal to:

$$\dot{Q}_{in} = \dot{m}_{src} c_{p,src} \left(T_{src,in} - T_{src,out}\right), \tag{A.6}$$

where $\dot{m}_{src}$, $c_{p,src}$ and $T_{source,in} - T_{source,out}$ are the heat-sink fluid mass flowrate, its specific heat capacity and its decrease in temperature in the evaporator, respectively. The working fluid specific enthalpy is raised to h_1, and $\dot{Q}_{in}$ is also equal to:

$$\dot{Q}_{in} = \dot{m}_{wf}(h_1 - h_4), \tag{A.7}$$

The energy balance, taking into account the heat output from the condenser, heat input in the evaporator, and work input in the compressor, can be represented by the following equation:

$$\dot{Q}_{out} = \dot{Q}_{in} + \dot{W}_{comp}\ . \tag{A.8}$$

The heat pump COP is obtained by dividing the heat transfer rate from the condenser to the heat-sink fluid, $\dot{Q}_{out}$, by the power input needed to operate the compressor, $\dot{W}_{comp}$:

$$\mathrm{COP} = \frac{\dot{Q}_{out}}{\dot{W}_{comp}}\ . \tag{A.9}$$

Appendix B. Costing correlations for heat pump components

The costing methodology used for the electric air-to-water heat pump is built upon the framework outlined in the authors' prior study [16]. The methodology involves the collection of cost data from various commercially available heat pump components on the UK market. The correlations established in this methodology initially covered plate and plate fin heat exchangers, the electric pump, the air fan, and the expansion valve. In this current study, the scope of these correlations has been expanded to encompass the three types of compressors under investigation: rotary-vane, scroll, and reciprocating-piston. The comprehensive set of correlations is presented in Table B1.

Table B1
Cost correlations for electric heat pump components.

Component	Dependent variable	Cost (£)
Condenser	Heat exchange area A_{cond} (m^2)	$288 + 316\ A_{cond}$
Evaporator	Heat exchange area A_{evap} (m^2)	$288 + 217\ A_{evap}$
Expansion valve	–	135
Air fan	Frontal area A_{fr} (m^2)	$578\ A_{fr}$
Pump	Work required $\dot{W}_{pump}$ (kW)	$512\ \dot{W}_{pump}^{0.46}$
Compressor (rotary-vane)	Inlet volumetric flowrate $\dot{V}_{comp,in}$ (m^3/s)	$8\,370\ \dot{V}_{comp,in}^{0.456}$
Compressor (scroll)	Inlet volumetric flowrate $\dot{V}_{comp,in}$ (m^3/s)	$166\,000\ \dot{V}_{comp,in}^{0.824}$
Compressor (piston)	Inlet volumetric flowrate $\dot{V}_{comp,in}$ (m^3/s)	$162\,000\ \dot{V}_{comp,in}^{0.839}$
Miscellaneous hardware	Total cost of components C_{tot}	$0.2\ C_{tot}$
Profit margin	Total cost of components C_{tot}	$0.2\ C_{tot}$
Tax	Total cost of components C_{tot}	$0.2\ C_{tot}$

Appendix C. Supplementary data

Supplementary data to this article can be found online at https://doi.org/10.1016/j.energy.2023.130171.

References

[1] Jakučionytė-Skodienė M, Krikštolaitis R, Liobikienė G. The contribution of changes in climate-friendly behaviour, climate change concern and personal responsibility to household greenhouse gas emissions: heating/cooling and transport activities in the European Union. Energy 2022;246:123387. https://doi.org/10.1016/j.energy.2022.123387.

[2] United Nations. Global status report for buildings and construction. 2021. https://globalabc.org/resources/publications/2021-global-status-report-buildings-and-construction.

[3] International Renewable Energy Agency. Renewable energy policies in a time of transition. 2021. https://www.irena.org/publications/2018/apr/renewable-energy-policies-in-a-time-of-transition.

[4] U.S. Energy Information Administration. Energy consumption by sector. 2022. https://www.eia.gov/totalenergy/data/annual.

[5] HM Government. Net zero Strategy: Build Back Greener. 2021. https://www.gov.uk/government/publications/net-zero-strategy.

[6] Olympios AV, Sapin P, Freeman J, Olkis C, Markides CN. Operational optimisation of an air-source heat pump system with thermal energy storage for domestic applications. Energy Convers Manag 2022;273:116426. https://doi.org/10.1016/j.enconman.2022.116426.

[7] International Energy Association. Energy prices: overview. 2022. https://www.iea.org/reports/energy-prices-overview.

[8] UK Parliament. Global net zero commitments. 2021. https://commonslibrary.parliament.uk/global-net-zero-commitments.

[9] Fischer D, Madani H. On heat pumps in smart grids: a review. Renew Sustain Energy Rev 2017;70:342–57. https://doi.org/10.1016/j.rser.2016.11.182.

[10] Tran CT, Rivière P, Waide P. Energy efficiency modelling of residential air source heat pump water heater. J. Sustain. Dev. Energy Water Environ. Syst. 2016;4(1):69–88. https://doi.org/10.13044/j.sdewes.2016.04.0007.

[11] Markides CN. The role of pumped and waste heat technologies in a high-efficiency sustainable energy future for the UK. Appl Therm Eng 2013;53:197–209. https://doi.org/10.1016/j.applthermaleng.2012.02.037.

[12] Palm B. Hydrocarbons as refrigerants in small heat pump and refrigeration systems - a review. Int J Refrig 2008;31(4):552–63. https://doi.org/10.1016/j.ijrefrig.2007.11.016.

[13] Gustafsson O, Teuillieres C, Hellgren H, Axell M, Dalenbäck JO. Reversing air-source heat pumps - noise at defrost initiation and a noise reducing strategy. Int J Refrig 2016;62:137–44. https://doi.org/10.1016/j.ijrefrig.2015.10.017.

[14] Schiffmann J, Favrat D. Design, experimental investigation and multi-objective optimization of a small-scale radial compressor for heat pump applications. Energy 2010;35(1):436–50. https://doi.org/10.1016/j.energy.2009.10.010.

[15] Olympios AV, Mersch M, Sapin P, Pantaleo MA, Markides CN. Library of price and performance data of domestic and commercial technologies for low-carbon energy systems (1.02. 2021. https://doi.org/10.5281/zenodo.5758943 [Data set].

[16] Olympios AV, Aunedi M, Mersch M, Krishnaswamy A, Stollery C, Pantaleo AM, Sapin P, Strbac G, Markides CN. Delivering net-zero carbon heat: technoeconomic and whole-system comparisons of domestic electricity- and hydrogen-driven technologies in the UK. Energy Convers Manag 2022;262:115649. https://doi.org/10.1016/j.enconman.2022.115649.

[17] Song L, Zeng L, Zhou J, Luo X. Profile design for the cylinder of a double-acting rotary vane compressor. Proc IME C J Mech Eng Sci 2016;230(13):2300–13. 10.1177%2F0954406215592923.

[18] Vodicka V, Novotny V, Zeleny Z, Mascuch J, Kolovratnik M. Theoretical and experimental investigations on the radial and axial leakages within a rotary vane expander. Energy 2019;189:116097. https://doi.org/10.1016/j.energy.2019.116097.

[19] Bianchi G, Cipollone R. Theoretical modeling and experimental investigations for the improvement of the mechanical efficiency in sliding vane rotary compressors. Appl Energy 2015;142:95–107. https://doi.org/10.1016/j.apenergy.2014.12.055.

[20] Gu H, Zhou X, Chen Y, Wu J, Wu Z, Jiang Y, Sundén B. Analysis, modeling and simulations of an innovative sliding vane rotary compressor with a rotating cylinder. Energy Convers Manag 2021;230:113822. https://doi.org/10.1016/j.enconman.2020.113822.

[21] Bianchi G, Rane S, Kovacevic A, Cipollone R, Murgia S, Contaldi G. Development of a general numerical methodology for CFD analyses in sliding vane machines and application on a mid-size oil injected air compressor. In: International compressor Engineering Conference; 2016. Paper 2454.

[22] Ba DC, Deng WJ, Che SG, Li Y, Guo HX, Li N, Yue XJ. Gas dynamics analysis of a rotary compressor based on CFD. Appl Therm Eng 2016;99:1263–9. https://doi.org/10.1016/j.applthermaleng.2016.01.062.

[23] Bianchi G, Cipollone R. Friction power modeling and measurements in sliding vane rotary compressors. Appl Therm Eng 2015;84:276–85. https://doi.org/10.1016/j.applthermaleng.2015.01.080.

[24] Bitzer. Scroll compressors. 2022. https://www.bitzer.de/gb/en/scroll-compressors.

[25] Energy International. Japanese and American competition in the development of scroll compressors and its impact on the American air-conditioning industry. Pacific Northwest Laboratory; 1990. https://digital.library.unt.edu/ark:/67531/metadc1190790.

[26] Byrne P, Ghoubali R, Miriel J. Scroll compressor modelling for heat pumps using hydrocarbons as refrigerants. Int J Refrig 2014;41:1–13. https://doi.org/10.1016/j.ijrefrig.2013.06.003.

[27] Wang X, Hwang Y, Radermacher R. Two-stage heat pump system with vapor-injected scroll compressor using R410A as a refrigerant. Int J Refrig 2009;32(6):1442–51. https://doi.org/10.1016/j.ijrefrig.2009.03.004.

[28] Ma GY, Zhao HX. Experimental study of a heat pump system with flash-tank coupled with scroll compressor. Energy Build 2008;40(5):697–701. https://doi.org/10.1016/j.enbuild.2007.05.003.

[29] Aprea C, Mastrullo R, Renno C. Experimental analysis of the scroll compressor performances varying its speed. Appl Therm Eng 2006;26(10):983–92. https://doi.org/10.1016/j.applthermaleng.2005.10.023.

[30] Shungarov EK, Garanov SA. Comparison of the characteristics of low-temperature scroll compressors for heat pump applications. Chem Petrol Eng 2020;56:378–84. https://doi.org/10.1007/s10556-020-00784-x.

[31] Gużda A, Szmolke N. Compressors in heat pumps. Mach. Dyn. Res. 2015;39(2):71–83. https://api.semanticscholar.org/CorpusID:114624987.

[32] Wang Y, Song J, Chatzopoulou MA, Sunny N, Simpson MC, Wang J, Markides CN. A holistic thermoeconomic assessment of small-scale, distributed solar organic Rankine cycle (ORC) systems: comprehensive comparison of configurations, component and working fluid selection. Energy Convers Manag 2021;248:114618. https://doi.org/10.1016/j.enconman.2021.114618.

[33] Sapin P, Simpson MC, White AJ, Markides CN. Lumped dynamic analysis and design of a high-performance reciprocating-piston expander. In: Proceedings of ECOS 2017 - the 30th International Conference on efficiency, costs, Optimization, simulation and environmental impact of energy systems; July 2-6, 2017. San Diego, California.

[34] Pérez-Segarra CD, Rigola J, Sòria M, Oliva A. Detailed thermodynamic characterization of hermetic reciprocating compressors. Int J Refrig 2004;28(No.4):579–93. https://doi.org/10.1016/j.ijrefrig.2004.09.014.

[35] Simpson M. On loss characterisation and minimisation in high-performance reciprocating-piston expanders. PhD Thesis. Imperial College London; 2021.

[36] Mathie R, Markides CN, White AJ. A framework for the analysis of thermal losses in reciprocating compressors and expanders. Heat Transf. Eng. 2014;35(16–17):1435–49. https://doi.org/10.1080/01457632.2014.889460.

[37] Willich C, Markides CN, White AJ. An investigation of heat transfer losses in reciprocating devices. Appl Therm Eng 2017;111:903–13. https://doi.org/10.1016/j.applthermaleng.2016.09.136.

[38] Taleb AI, Barfuß C, Sapin P, White AJ, Fabris D, Markides CN. Simulation of thermally induced thermodynamic losses in reciprocating compressors and expanders: influence of real-gas effects. Appl Therm Eng 2022;217:118738. https://doi.org/10.1016/j.applthermaleng.2022.118738.

[39] Song J, Olympios AV, Mersch M, Sapin P, Markides CN. Integrated organic Rankine cycle (ORC) and heat pump (HP) systems for domestic heating, Proceedings of ECOS 2021 - the 34th International Conference on efficiency, costs, Optimization, simulation and environmental impact of energy systems, Taormina, Italy. 2021. June 28-July 2.

[40] Pantaleo AM, Simpson M, Rotolo G, Distaso E, Oyewunmi OA, Sapin P, De Palma P, Markides CN. Thermoeconomic optimisation of small-scale organic Rankine cycle systems based on screw vs. piston expander maps in waste heat recovery applications. Energy Convers Manag 2019;200:112053. https://doi.org/10.1016/j.enconman.2019.112053.

[41] Lemort V, Declaye S, Quoilin S. Experimental characterization of a hermetic scroll expander for use in a micro-scale Rankine cycle. Proc Inst Mech Eng A J Power Energy 2012;226(1):126–36. 10.1177%2F0957650911413840.

[42] Astolfi M. Techno-economic optimization of low temperature CSP systems based on ORC with screw expanders. Energy Proc 2015;69:1100–12. https://doi.org/10.1016/j.egypro.2015.03.220.

[43] Simpson MC, Rotolo G, Sapin P, De Palma P, White AJ, Markides CN. Thermodynamic performance maps of reciprocating-piston expanders for operation at off-design and part-load conditions. In: Proceedings of HEFAT 2017 - the 13th International Conference on heat transfer. Portorož, Slovenia: Fluid Mechanics and Thermodyamics; July .

[44] Lemort V, Guillaume L, Legros A, Declaye S, Quiilin S. A comparison of piston, screw and scroll expanders for small-scale Rankine cycle systems. In: Proceedings of MICROGEN III - the 3rd International Conference on Microgeneration and related technologies. Naples, Italy; 2013. April 14-17.

[45] Glavatskaya Y, Podevin P, Lemort V, Shonda O, Descombes G. Reciprocating expander for an exhaust heat recovery Rankine cycle for a passenger car application. Energies 2012;5(6):1751–65. https://doi.org/10.3390/en5061751.

[46] Air-conditioning. Heating and Refrigeration Institute. Standard for performance rating of positive displacement refrigerant compressors. 2020. https://www.ahrinet.org/search-standards.

[47] Zhao LX, Zhang CL, Gu B. Neural-network-based polynomial correlation of single- and variable-speed compressor performance. HVAC R Res 2009;15(2):255–68. https://doi.org/10.1080/10789669.2009.10390836.

[48] Bitzer. BITZER Software v6.17.7. 2022. https://www.bitzer.de/websoftware.

[49] Area cooling Solutions. Compressors; 2022. https://areacooling.com/c/compressors.

[50] Lemmon EW, Huber ML, McLinden MO. NIST standard reference database 23: reference fluid thermodynamic and transport properties - REFPROP. 2013., Version 9.1. https://www.nist.gov/publications/nist-standard-reference-database-23-reference-fluid-thermodynamic-and-transport.

[51] The Mathworks. MATLAB R2022a. 2022. https://uk.mathworks.com/products/matlab.html.

[52] Mitsubishi Electric. Ecodan monobloc air source heat pumps. 2022. https://les.mitsubishielectric.co.uk/products/residential-heating/outdoor.

[53] Panasonic. Aquarea high performance all in one compact. 2022. https://www.aircon.panasonic.eu/GB_en/ranges/aquarea/high-performance.

[54] Global Modeling and Assimilation Office, MERRA-2 inst3_3d_asm_Np: 3d, 3-hourly, instantaneous, pressure-level, assimilation, assimilated meteorological fields V5.12.4. Greenbelt, MD, USA: Goddard Earth Sciences Data and Information Services Centre (GES DISC); 2015. https://doi.org/10.5067/QBZ6MG944HW0.

[55] Chartered Institution of Building Services Engineers, Guidance note: domestic hot water temperatures from instantaneous heat interface units. 2021. https://www.cibse.org/knowledge-research/knowledge-portal/guidance-note-domestic-hot-water-temperatures-from-instantaneous-heat-interface-units.

[56] National House Building Council. Underfloor heating: a guide for house builders. 2016. https://www.nhbcfoundation.org/wp-content/uploads/2016/09/NF71-Guide-to-Underfloor-Heating.pdf.

[57] Underfloor heating systems Ltd. What is the water flow temperature? 2023. https://www.underfloorheatingsystems.co.uk/self-install-information/questions-and-answers/what-is-the-water-flow-temperature.

[58] Wang JF, Brown C, Cleland DJ. Heat pump heat recovery options for food industry dryers. Int J Refrig 2018;86:48–55. https://doi.org/10.1016/j.ijrefrig.2017.11.028.

[59] Yu B, Ouyang H, Shi J, Liu W, Chen J. Evaluation of low-GWP and mildly flammable mixtures as new alternatives for R410A in air-conditioning and heat pump system. Int J Refrig 2021;121:95–104. https://doi.org/10.1016/j.ijrefrig.2020.09.018.

[60] Environmental Protection Agency. Protection of stratospheric ozone: Revisions to the refrigerant management program's extension to substitutes. 2020. https://www.federalregister.gov/documents/2020/03/11/2020-04773/protection-of-stratospheric-ozone-revisions-to-the-refrigerant-management-programs-extension-to.

[61] Chen W. A comparative study on the performance and environmental characteristics of R410A and R22 residential air conditioners. Appl Therm Eng 2008;28(1):1–7. https://doi.org/10.1016/j.applthermaleng.2007.07.018.

[62] Bolaji BO, Huan Z. Ozone depletion and global warming: case for the use of natural refrigerant – a review. Renew Sustain Energy Rev 2013;18:49–54. https://doi.org/10.1016/j.rser.2012.10.008.

[63] British Standards Institution, BS EN 14511-4: 2018: air conditioners, liquid chilling packages and heat pumps for space heating and cooling and process chillers, with electrically driven compressors. 2018. https://www.thenbs.com/PublicationIndex/documents/details?Pub=BSI&DocID=322297.

[64] Olympios AV, Pantaleo AM, Sapin P, Markides CN. On the value of combined heat and power (CHP) systems and heat pumps in centralised and distributed heating systems: Lessons from multi-fidelity modelling approaches. Appl Energy 2020;274:115261. https://doi.org/10.1016/j.apenergy.2020.115261.

[65] International Energy Agency. Projected costs of generating electricity. 2020. https://www.iea.org/reports/projected-costs-of-generating-electricity-2020.

[66] De La Torre C, Martinez R, Lemmon A. Understanding the discounted payback technique and its uses for small business. 2016. https://academyfinancial.org/resources/Documents/Proceedings/2016/7C-Torre.pdf.

[67] Department of Business Energy & Industrial Strategy. Cost of installing heating measures in domestic properties. 2018. https://www.gov.uk/government/publications/cost-of-installing-heating-measures-in-domestic-properties.

[68] Local Heros. How much does a boiler service cost?. 2022. https://www.localheroes.com/advice/how-much-boiler-service.

[69] International Energy Agency. Levelised cost of heating for air-to-air and air-to-water heat pumps and gas boilers for selected countries, and sensitivity to fuel prices H1 2021 - H1 2022. 2022. https://www.iea.org/data-and-statistics/charts/levelised-cost-of-heating-for-air-to-air-and-air-to-water-heat-pumps-and-gas-boilers-for-selected-countries-and-sensitivity-to-fuel-prices-h1-2021-h1-2022.

[70] Sansom R. Decarbonising low grade heat for low carbon future, Ph. D. Thesis, Imperial College London, Ankara. 1983. https://doi.org/10.25560/25503.

[71] Ruhnau O, Hirth L, Praktiknjo A. Time series of heat demand and heat pump efficiency for energy system modeling. Sci Data 2019;6:189. https://doi.org/10.1038/s41597-019-0199-y.

[72] Aunedi M, Olympios AV, Pantaleo AM, Markides CN, Strbac G. System-driven design and integration of low-carbon domestic heating technologies. Renew Sustain Energy Rev 2023;187:113695. https://doi.org/10.1016/j.rser.2023.113695.

[73] Department for Energy Security and Net Zero. Energy price guarantee: regional rates. 2023. https://www.gov.uk/government/publications/energy-price-guarantee-regional-rates.

[74] Global Petrol Prices. Finland fuel prices, electricity prices.; 2023. https://www.globalpetrolprices.com/Finland/.

[75] Global Petrol Prices. Greece fuel prices. electricity prices, natural gas prices.; 2023. https://www.globalpetrolprices.com/Greece/.